Supporting Information

Topological Regulation in Polysilsesquioxanes for Achieving Super-Hard and Flexible Membranes: Insights from Molecular Simulation

Peng Xu [# 1, 2], Yuxin Sun [# 2], Song Yang [2], Guangxin Chen [2], Jiali Qu [2], Qifang Li * [2], and Zheng Zhou * [1,2]

1 P. Xu, Prof. Dr. Z. Zhou
Key Laboratory of Carbon Fiber and Functional Polymers, Ministry of Education
Beijing University of Chemical Technology
Beijing 100029, China
E-mail: zhouzheng@mail.buct.edu.cn; qflee@mail.buct.edu.cn

2 P. Xu, Y.-X. Sun, S. Yang, Prof. Dr. G.-X. Chen, Dr. J.-L Qu, Prof. Dr. Q.-F. Li, Prof. Dr. Z. Zhou
College of Material Science and Engineering
Beijing University of Chemical Technology
Beijing 100029, China

# These authors contribute equally to this work.

Materials and methods

Materials.2-(3,4-epoxycyclohexyl) ethyl trimethoxysilane, K_2CO_3, photoinitiator (Irgacure250) were purchased from Beijing Inokai Technology Co. EPOSS were prepared in-house [36].

Synthesis of ELPSQ. A mixture of H_2O (12g, 0.67mol) and DCM (20g, 0.28mol), and KOH (0.1g, 7.2×10-4mol) were added and stirred thoroughly in a dry three-necked flask. Subsequently, 2-(3,4-epoxycyclohexyl) ethyl trimethoxysilane(49.28g, 0.2mol) was added dropwise, and the reaction was conducted at room temperature for 28 hours. A transparent viscous liquid, ladder-like polysilsesquioxane with cyclohexyl epoxy groups (ELPSQ), was obtained after evaporating the solvent using rotary evaporation at a yield of 95.52%.

Preparation of EPOSS-reinforced ELPSQ resin membranes. The glass slide and polyimide (PI) membrane were ultrasonicated in a water bath for 10 min using acetone, deionized water, and anhydrous ethanol in turn. Subsequently, air-dried in air after being cleaned for subsequent use. The preparation process of the EPOSS-reinforced ELPSQ resin membranes (PL resin membranes) is illustrated in **Figure 1a**. According the formula in Table 1, a certain mass fraction of ELPSQ and EPOSS was weighed in a beaker, and then 10 mL of tetrahydrofuran and 0.12 g of photoinitiator (Irgacure250) were added. The mixture was then stirred well on a magnetic stirrer. The samples were scrape-coated onto slides and PI membrane substrates using a computerized coater at 200 mm/min. The substrates coated with the samples were placed in a light-proof oven at 60 °C to evaporate the solvents to remove the solvents, and the curing process was completed by UV irradiation under nitrogen atmosphere for 20 min. For ease of documentation, the samples were named EP-0, EP-10, EP-20, and EP-100 according to the amount of EPOSS added to the resin system.

Measurements

^{1}H NMR and ^{29}Si NMR spectra were recorded by a Bruker AV 11-400 spectrometer in the 400 MHz range in $CDCl_3$ (0.05% TMS as an internal standard) at room temperature.

Fourier-transform infrared (FTIR) spectroscopic analysis was performed through Bruker Tensor 27 spectrometer (Bruker Optics Inc.) by using pellets in transmission mode in the range of 4000 cm^{-1} to 400 $cm^{-1}$with 32 scans.

The sample was prepared into 5 mg/ml THF solution, and then the molecular weight was tested with THF as the mobile phase and 40℃ as the test temperature.

The Ultima IV X-ray diffraction analyzer was used to analyze the structure of the sample. The test radioactive source is a Cu Kα ray with a wavelength of 0.154 nm, the scanning test range(2θ) is 5 ~ 90°, and the scanning rate is 6 °/min.

MIRA LMS scanning electron microscope (field emission) and Xplore EDS spectrometer of TESCAN were used to analyze the micromorphology and element distribution of UV-curable silicone resin samples.

The epoxy conversion of the resin membrane was tested using a real-time infrared spectrometer (Nicole 5700 FTIR type) to analyze the polymerization rate of the resin during the photocuring process. The area of the epoxy peak at 885 cm^{-1} was monitored in real time, and the conversion rate of the epoxy group was calculated by the change of the area of the epoxy group peak.

The light transmittance of the sample was measured on the glass slide and the resin-coated glass slide on the fog meter (type TH-110). The absorbance of the glass coated with resin was tested by UV-1800 spectrophotometer with a scanning range of 300 ~ 900 nm, and the light transmittance of the sample was calculated according to Beer's law.

The scratch resistance of the resin membrane was tested according to ASTM test standards, and the pencil hardness grades from hard to soft were 9H, 8H, 7H, 6H, 5H, 4H, 3H, 2H, H, F, HB, B, 2B, 3B, 4B, 5B, 6B, 7B, 8B, 9B. Load the pencil into the pencil hardness tester (QHQ-A), forming a 45° Angle with the coated surface, and move the pencil forward. The pencil hardness of the membrane is the maximum hardness level that does not leave a scratch on the resin membrane.

The resin membrane was tested using a nanoindenter (Burker Hysitron TI980) equipped with a diamond Berkovich indenter with loading and unloading times of 15 s and a maximum load holding time of 15 s. The indentation hardness, modulus and elastic recovery rate were calculated by using the Oliver Pharr method. The nanoindentation hardness of the resin membrane was characterized by two measurement modes: positioning and fixed load. In order to prevent the influence of the substrate on the hardness measurement of the resin membrane, the maximum indentation depth in the test process should be less than 10% of the membrane thickness.

The surface morphology and roughness of the resin membrane were measured using Bruker Dimension Icon Atomic force microscope (AFM).

Friction and wear testing machine (SRV-IV) was used to test the wear of the resin membrane. Wrap the steel wool mesh (grade #0000) around the end of the metal latch. Assuming that the steel wool is in full contact with the membrane, the average vertical pressure exerted by the steel wool on each sample is 5.2 N, the diameter of the wear probe is 16 mm, and the probe travels 20 mm in each wear stroke. After 100, 200 and 300 times of wear, the membrane morphology was photographed by polarizing microscope (Leica DM4P model).

In accordance with ISO 1519:2011, the bending properties of the membrane were tested using a cylindrical bending tester (QTY-32). The resin is coated on 50 μm thick PI membranes, which will cure, and the membranes are bent tightly on mandrel diameters of 32, 25, 20, 16, 12, 10, 8, 6, 5, 4, 3, and 2 mm. The minimum radius of curvature of the sample is the minimum or critical bending diameter of the mandrel on which the resin membrane can bend but is not cracked.

According to literature [37], a bending test model was made by ourselves. The production process was as follows: two parallel glass slides were glued with tape to form a hinge. The rubber sheets of 8 mm, 6 mm, 4 mm and 2 mm thickness are sandwiched between parallel slides. Before the bending test, the resin-coated PI membrane was fitted tightly with tape between two slides. When the hinge is open, the membrane is flat; When the hinge is closed, the membrane is folded into a nearly semi-circle shape. In this way, a bending cycle is completed in about 30 seconds. After repeating the bending cycle for five times, the PI membrane coated with resin was removed and the damage of the membrane was observed with the naked eye and microscope.

The coatings were subjected to repeated thermal cycling between extreme temperatures to assess their resistance to thermal stress. Samples were alternated between −40 °C for 2 hours and 85 °C for 2 hours over 20 cycles. Compare the change of light transmittance before and after the test to ensure theirs stability under harsh environmental conditions.

The corrosion resistance of the coatings was tested using a salt spray chamber (ASTM B117 standard). Samples were exposed to a 5% NaCl solution at 35 °C for 72 hours. After exposure, the coatings were inspected for corrosion, blistering, or peeling, providing insights into their durability in saline environments.

The thermal stability of the coatings was evaluated using thermogravimetric analysis. Samples were heated under a nitrogen atmosphere at a rate of 10 °C/min from room temperature to 800 °C. The weight loss curves were recorded to determine the decomposition temperature and thermal resistance of the materials, providing a deeper understanding of their durability under high-temperature conditions.

The adhesion of the coating to the substrate was assessed using the cross-cut adhesion test (ISO 2409 standard). A grid of 1 mm × 1 mm squares was cut into the coating using a sharp blade, followed by the application of adhesive tape. The adhesion was rated based on the degree of coating removal after peeling off the tape, with classifications ranging from 0 (no detachment) to 5 (significant detachment). This test provided insights into the bonding strength between the coating and the substrate.

Molecular dynamics simulation

Establishment of molecular dynamics model of PL resin membranes. The molecular dynamics model of PL resin membrane is depicted in Figure 6a, b. Initially, the EPOSS molecule and ELPSQ molecule were constructed manually and then their structures were optimized. The amorphous Cell module was utilized to package the two molecules in different proportion, with a density of 0.5 g/cm^3. Subsequently, models with EPOSS content of 0%, 10%, 20% and 100% were respectively constructed.

Next, the Forcite module was utilized for geometric optimization with a duration of 100000 ps. Subsequently, the Dynamics task within the module was employed to select the NVT assembly for two rounds of regular system optimization at a temperature of 298 K and for a duration of 200 ps in order to achieve equilibrium duration of 200 ps. The model optimization then proceeded with the cyclic "annealing" operation using the Forcite module. The Anneal task was used to select the NVT assembly with a minimum temperature of 300 K and a maximum temperature of 700K, with steps balanced every 20 K over a total of 80,000 kinetic steps across ten cycles. The cycle resulting in the lowest energy at its conclusion was selected, and the corresponding model from that cycle's motion trajectory file was determined. The annealed model underwent further optimization using the Dynamics task within the module, selecting an NPT ensemble at a temperature of 298K and pressure of 0.01 GPa for another duration of 200 ps. These steps were repeated until system energy met balance requirements, yielding a fully balanced model ready for subsequent calculation and analysis.

Molecular dynamics calculation. The 'Mechanical Properties' tool in the Forcite module of Materials Studio software was used to implement the constant stress-strain fluctuation method. The step length was set to 5, with a maximum strain amplitude of 0.003. The mechanical properties of EP-0, EP-10, EP-20, and EP-100 were analyzed separately. The Conformers module in Materials studio is used to build the relationship between O-Si-C-C torsion Angle and rotational energy barrier in EPOSS and ELPSQ monomer. The STEP value is changed to 72, the Interval to 5, and Universal force field is used. The Dynamics task in Forcite module in Materials studio software was

used to select NVT components, and the system was optimized at 298 K temperature and 500 ps duration. After optimization, the result file was analyzed, and Mean square displacement was selected. The mean azimuth shift of EP-0, EP-10, EP-20 and EP-100 PL resin systems at 298 K was calculated.

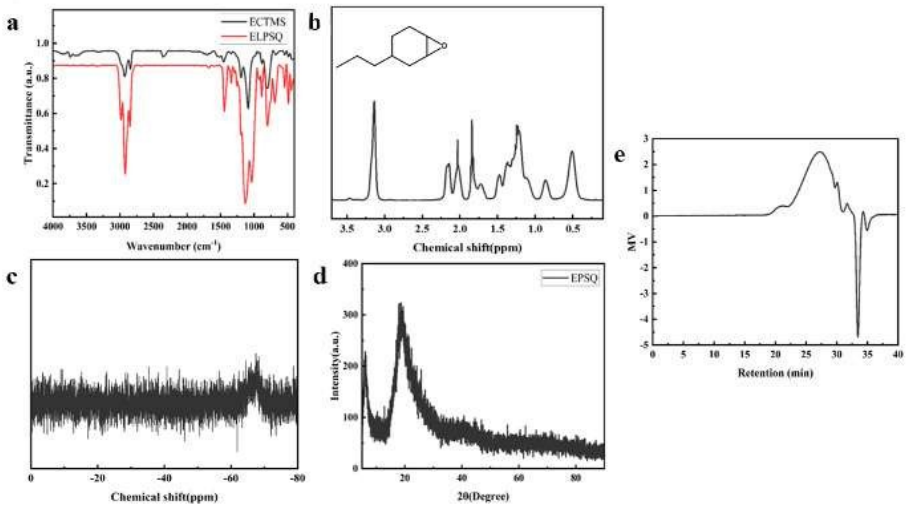

Figure S1. Structural characterization of ELPSQ: a)FTIR spectra, b)^{1}H NMR spectrum, c)^{29}SiNMR spectrum, d)XRD spectrum and e)GPC outflow curve

Table S1 The statistical results of GPC tests of EPSQ

Broad Unknown Relative Peak Table

	Distribution Name	Mn (Daltons)	Mw (Daltons)	MP (Daltons)	Mz (Daltons)	Mz+1 (Daltons)	Polydispersity	Mz/Mw	Mz+1/Mw
1		112276	129956	90224	154913	186843	1.157467	1.192048	1.437743
2		5201	11416	5348	22963	35139	2.195015	2.011533	3.078164
3		1013	1033	1000	1054	1075	1.020536	1.020133	1.039839

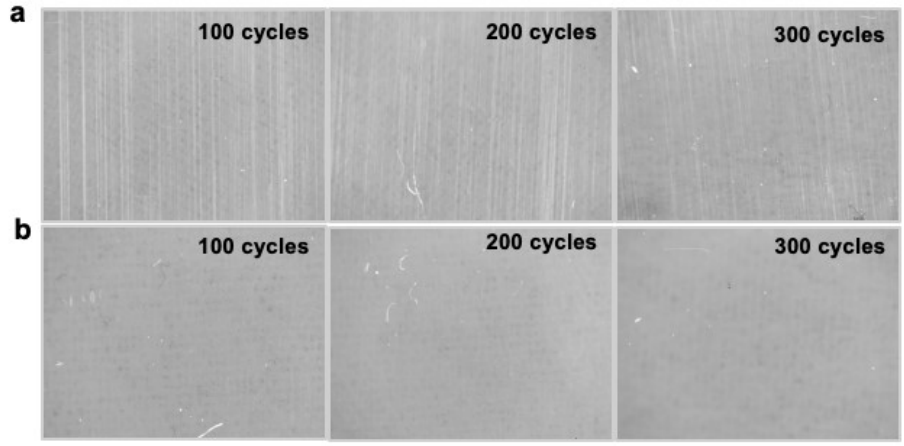

Figure S2. Microscope image of PI and EP-10 resin membrane after friction and wear: a) images of PI after 100, 200, 300 friction cycles, b) images of EP-10 resin membrane after 100, 200, 300 friction cycles

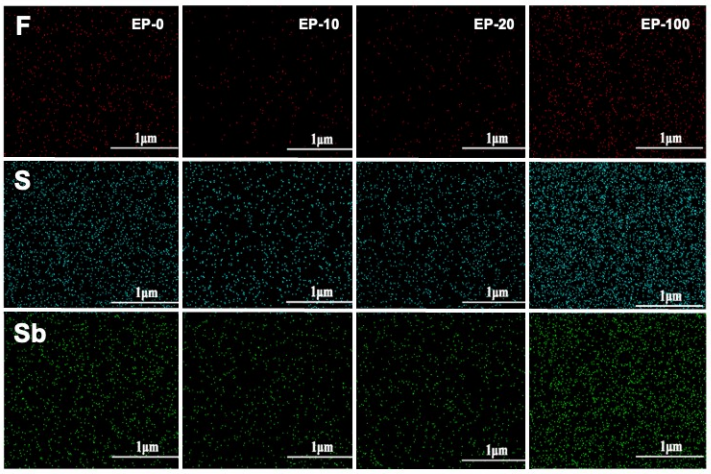

Figure S3. Cross-section elemental analysis of PL resin membranes: EP-0, EP-10, EP-20, EP-100

Table S2 The mechanical properties of the various coatings samples measured via nanoindentation.

sample	E[a](GPa)	H[a](GPa)	We[a](%)
EP-0	12.68±0.12	1.45±0.01	0.84±0.06
EP-10	13.83±0.14	1.56±0.01	0.88±0.04
EP-20	12.90±0.02	1.40±0.01	0.93±0.02
EP-100	12.45±0.15	1.37±0.02	0.90±0.02

a.The numbers after the ± signs are the standard deviations.

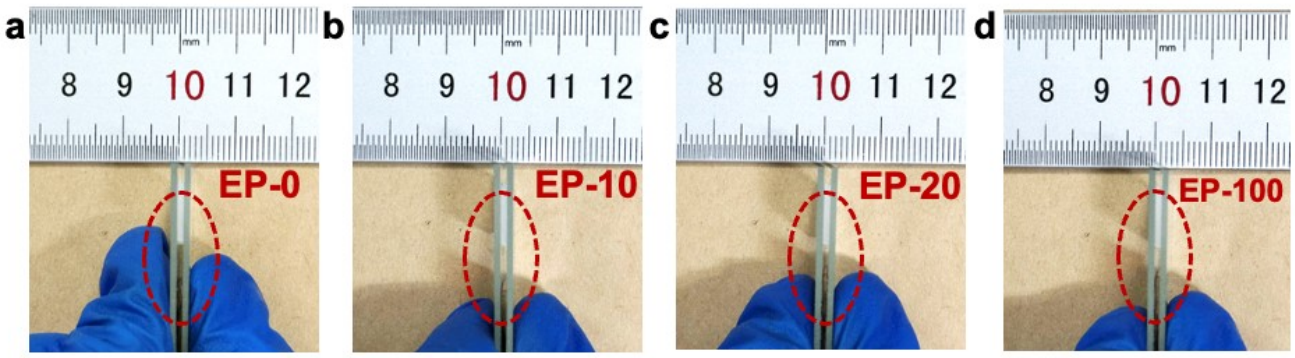

Figure S4. Test diagrams of curvature radius of a) EP-0, b) EP-10, c) EP-20 and d) EP-100;

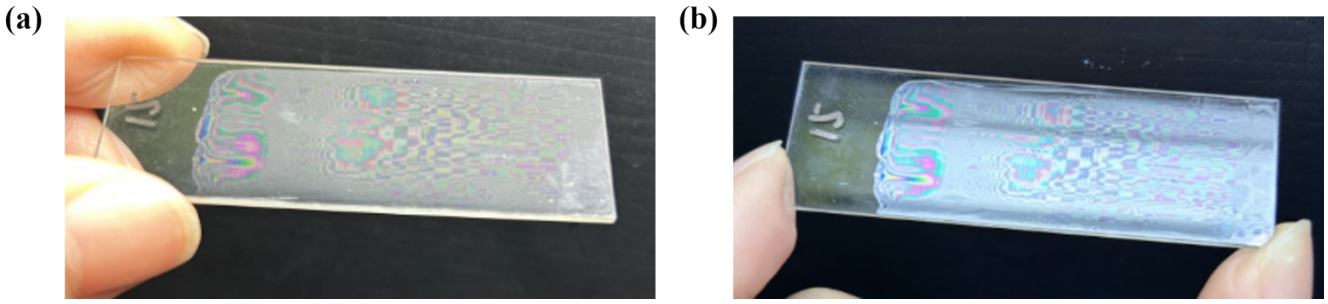

Figure S5. a) Before the thermal cycling test;b) After the thermal cycling test

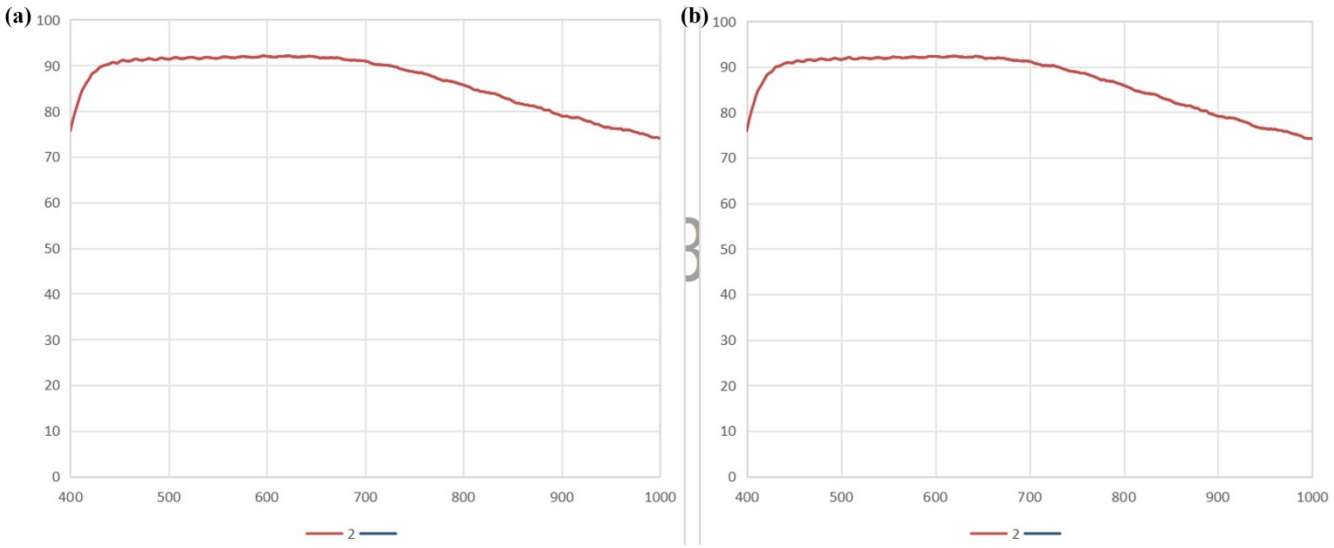

Figure S6. a)The transmittance before the thermal cycling tes;b) The transmittance after the thermal cycling test

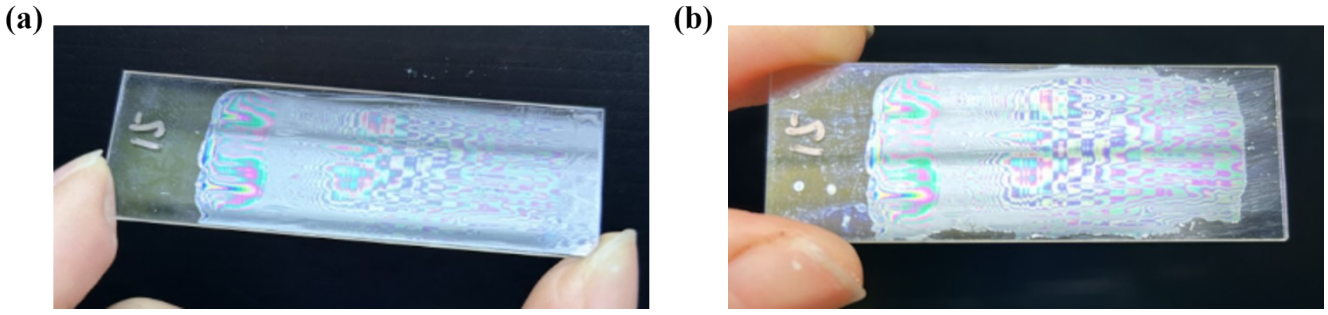

Figure S7. a) Before the salt spray test;b) After the salt spray test

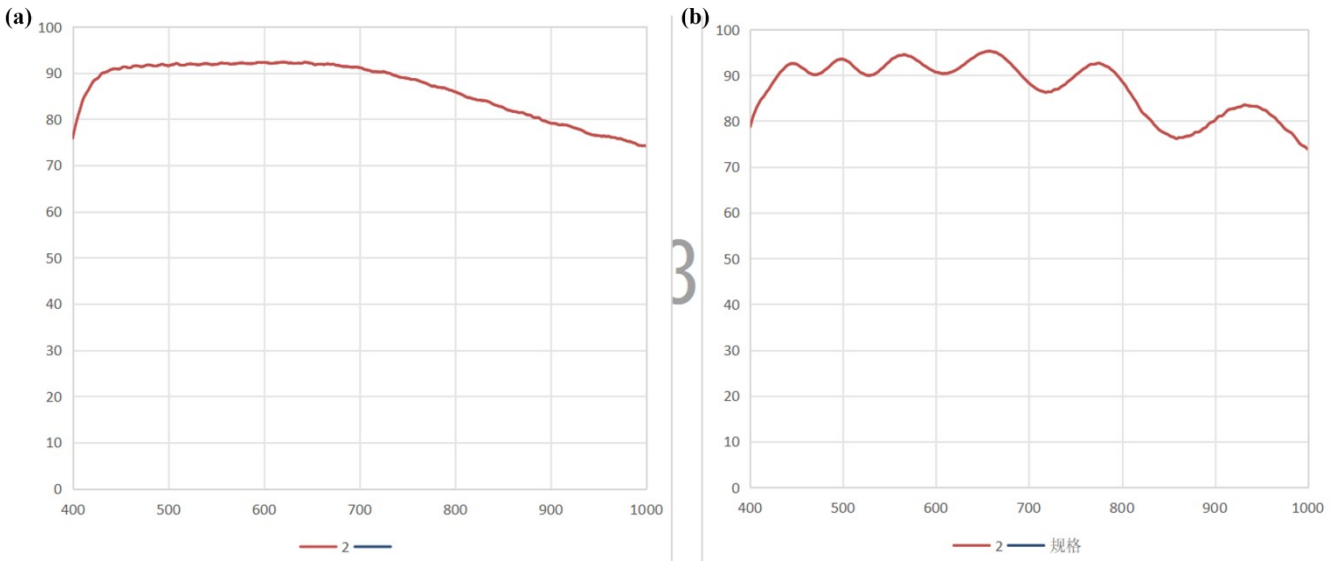

Figure S8. a)The transmittance before the salt spray test;b) The transmittance after the salt spray test

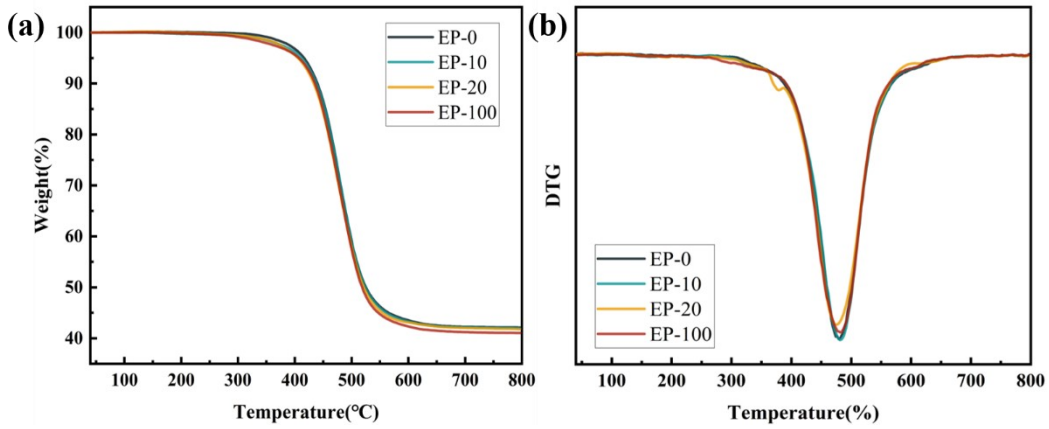

Figure S9 Thermogravimetric curve of PL resin coating under nitrogen atmosphere: (a)TG and (b)DTG

Table S3 TG date of PL resin coating under nitrogen atmosphere

sample	Td5%/℃	Td10%/℃	Tmax/℃	R800℃/%
EP-0	416.3	439.8	479.6	42.11
EP-10	412.2	438.4	482.1	41.96
EP-20	405.6	433.3	475.5	41.86
EP-100	407.4	435.5	479.6	41.04

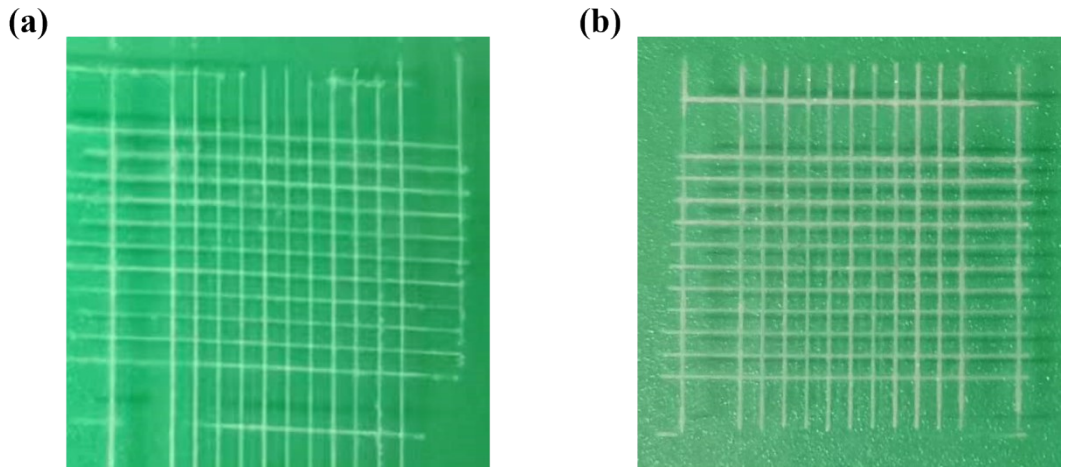

Figure S10 a)The adhesion of the coating on PC substrate was measured by the cross-cut test; (b) The adhesion of the coating on PMMA substrate was measured by the the cross-cut test

Table S4. Elastic rigid matrix of EP-0 system

Cij/GPa Error/GPa	1	2	3	4	5	6
1	83.7451 ±2.0818	45.3864 ±2.3471	28.1327 ±2.2738	-4.8581 ±1.8262	-5.7069 ±1.8328	-10.1816 ±2.4069
2	0	55.142 ±2.7756	31.4363 ±2.4891	-9.4693 ±2.0389	0.0675 ±2.0867	-9.9841 ±2.8821
3	0	0	153.8214 ±2.9226	-8.0340 ±2.2270	-8.3843 ±1.9940	5.0716 ±2.7811
4	0	0	0	23.3215 ±1.7432	6.8259 ±1.5907	-0.6302 ±2.2237
5	0	0	0	0	23.9173 ±1.6402	-2.0099 ±2.1278
6	0	0	0	0	0	36.1666 ±3.2131

Table S5. Elastic rigid matrix of EP-10 system

Cij/GPa Error/GPa	1	2	3	4	5	6
1	94.5191 ±2.1331	42.8094 ±3.1105	27.5979 ±2.4049	3.3548 ±2.2593	5.0272 ±1.6327	-9.1528 ±2.4519
2	0	109.7140 ±5.5606	27.0259 ±3.6970	10.5682 ±3.7169	1.5262 ±2.3562	2.7832 ±4.3637
3	0	0	78.0620 ±3.0928	11.0663 ±2.8290	5.5081 ±1.5115	5.1518 ±2.9030
4	0	0	0	41.7869 ±2.1784	3.8082 ±2.3055	12.4741 ±1.5452
5	0	0	0	0	24.1774 ±1.3721	2.8281 ±1.8734
6	0	0	0	0	0	32.9826 ±3.6060

Table S6. Elastic rigid matrix of EP-20 system

Cij/GPa Error/GPa	1	2	3	4	5	6
1	83.7451 ±2.0818	45.3864 ±2.3471	28.1327 ±2.2738	-4.8581 ±1.8262	-5.7069 ±1.8328	-10.1816 ±2.4069
2	0	55.142 ±2.7756	31.4363 ±2.4891	-9.4693 ±2.0389	0.0675 ±2.0867	-9.9841 ±2.8821
3	0	0	153.8214 ±2.9226	-8.0340 ±2.2270	-8.3843 ±1.9940	5.0716 ±2.7811
4	0	0	0	23.3215 ±1.7432	6.8259 ±1.5907	-0.6302 ±2.2237
5	0	0	0	0	23.9173 ±1.6402	-2.0099 ±2.1278
6	0	0	0	0	0	36.1666 ±3.2131

Table S7. Elastic rigid matrix of EP-100 system

Cij/GPa Error/GPa	1	2	3	4	5	6

1	151.2800 ±2.3768	34.3200 ±5.4509	34.9646 ±5.2302	-10.3248 ±5.4867	-14.8929 ±5.2348	8.9307 ±5.2178
2	0	103.1883 ±5.8305	28.0373 ±5.8567	-7.9018 ±5.2585	-12.1391 ±5.0007	8.7873 ±4.6372
3	0	0	60.3698 ±6.0781	-8.5552 ±5.3107	-9.2207 ±5.0878	2.1755 ±4.5091
4	0	0	0	26.7903 ±5.2703	5.8543 ±4.9195	-0.1217 ±4.6012
5	0	0	0	0	25.0104 ±4.8804	-1.6423 ±4.5701
6	0	0	0	0	0	44.3428 ±4.5035